

Semiannual patterns of erosion and deposition in upper Monterey Canyon from serial multibeam bathymetry

Douglas P. Smith[†]

Genoveva Ruiz[‡]

Rikk Kvitek[§]

Pat J. Iampietro[#]

Division of Science and Environmental Policy, California State University Monterey Bay, 100 Campus Center, Seaside, California 93933, USA

ABSTRACT

Recently acquired 3-m-resolution 244 kHz multibeam seafloor bathymetry (0.5 m depth precision) reveals geomorphology at sufficient detail to interpret small-scale features and short-term processes in the upper 4 km of Monterey Canyon, California. The study area includes the continental shelf and canyon features from 10 m to 250 m depth. The canyon floor contains an axial channel laterally bounded by elevated complex terrace surfaces. Sand waves with 2 m height and 35 m average wavelength dominate the active part of the canyon floor. The sand waves are strongly asymmetrical, indicating net down-canyon sediment transport in this reach. Terraces, including a broad 25-m-tall terrace complex near the head of the canyon, bear evidence of recent degradation of the canyon floor. Slump scars and gullies having a variety of sizes and relative ages shape the canyon walls. Serial georeferenced digital elevation models were analyzed to detect net changes in bathymetry or morphology occurring during both a six month period (September 2002 to March 2003) and a 24-h period (24 March to 25 March). Significant changes over the six month period include: (1) complete reorganization of the sand waves on the channel floor, (2) local channel degradation creating new 2-m-tall erosional terraces on the channel margins, (3) local channel widening that laterally eroded older channel margin terraces, and (4) 60 m extension of one minor gully head on a steep canyon wall. There were no discernable changes in morphology during the 24-h study period. Raster subtraction of

serial bathymetric grids provides estimates of sediment erosion and deposition that occurred between the canyon head and a point 2 km down canyon during the six month study. Erosion of 320,000 m³ ($\pm 80,000$ m³) of sediment occurred mainly in the tributaries, along the margins of the axial channel, and in the lowest 700 m of the analyzed reach. This eroded volume was approximately balanced by 260,000 m³ ($\pm 70,000$ m³) of sediment deposition that was concentrated in the nearshore region along the rim of the canyon head. There was no measurable sediment gain or loss during the 24-h study period.

Keywords: Monterey, submarine, canyon, sediment, morphology, bathymetry.

INTRODUCTION

Seafloor mapping and sedimentological studies of the continental shelf and submarine canyons of Monterey Bay, California, have provided a wealth of information about submarine canyon processes and the tectonic history of coastal California (Fig. 1). Recent studies of high-resolution single beam and multibeam bathymetric data provide detailed interpretations of the tectonics, structure, geology, and

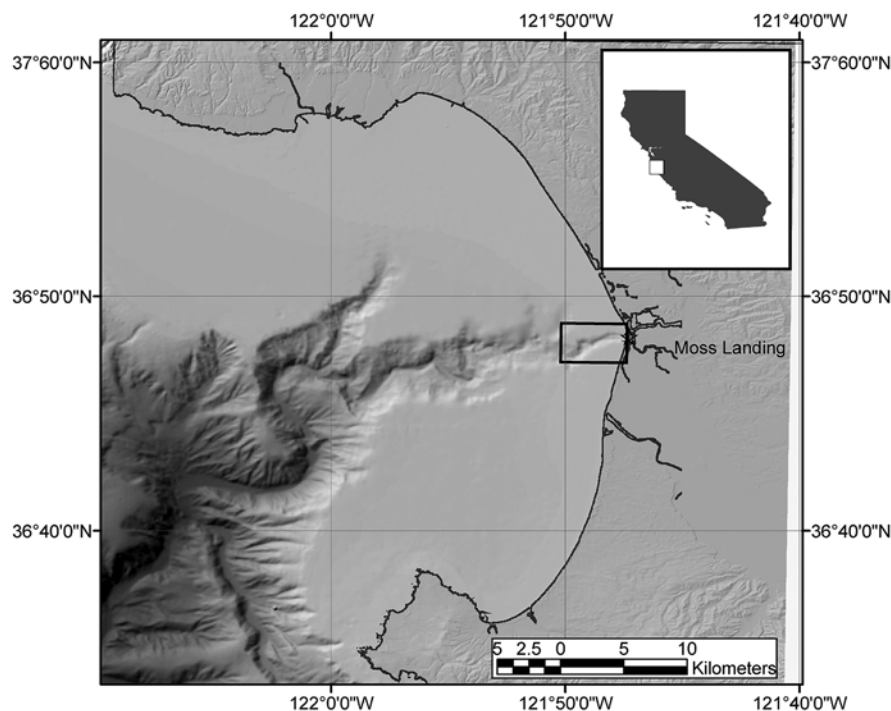


Figure 1. Digital image of terrestrial and submarine continental margin at Monterey Bay, California. Small box shows study area and location of Figures 2 and 3.

[†]E-mail: douglas_smith@csumb.edu.

[‡]E-mail: genoveva_ruiz@csumb.edu.

[§]E-mail: rikk_kvitek@csumb.edu.

[#]E-mail: pat_iampietro@csumb.edu.

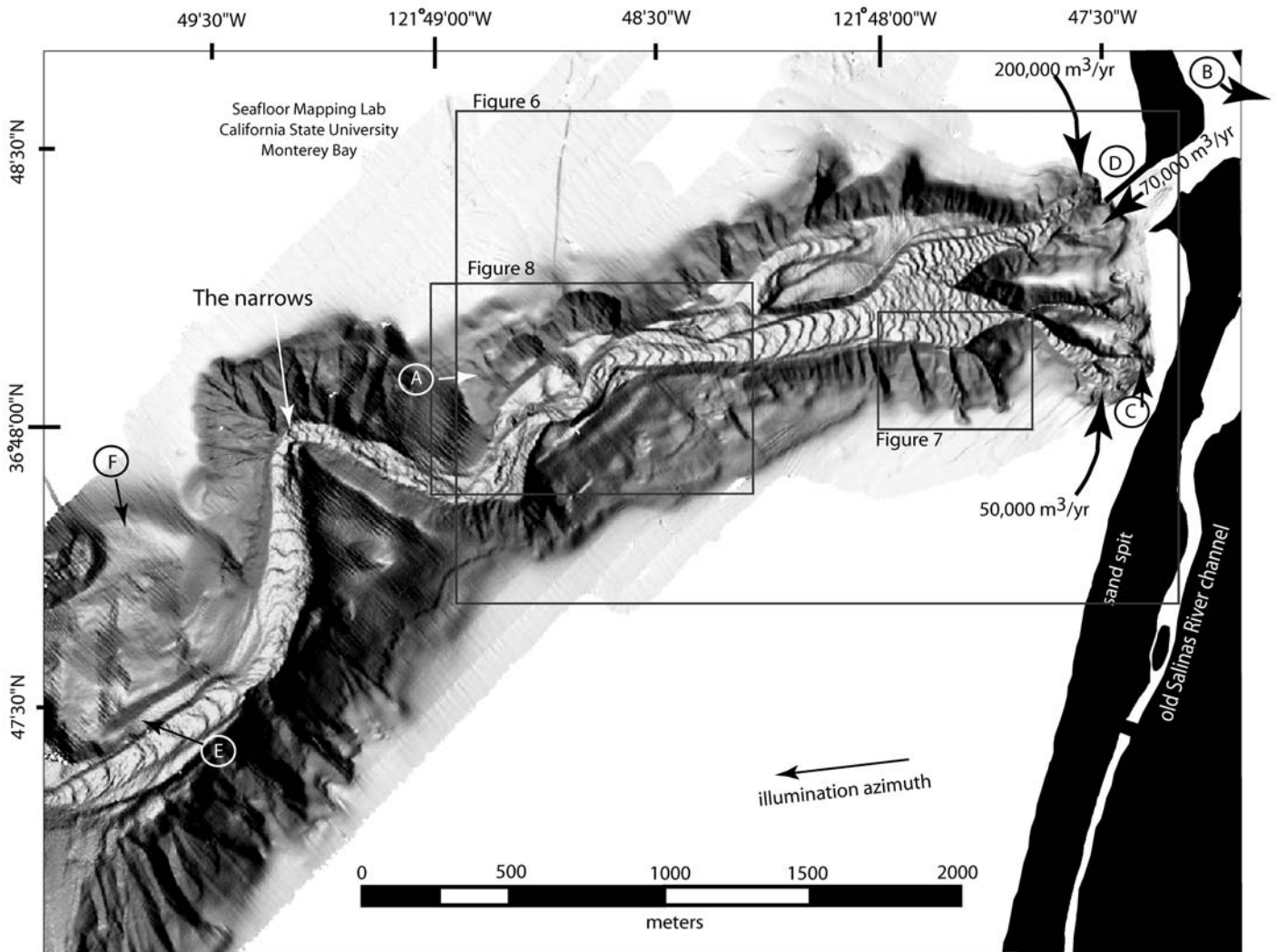


Figure 2. Three-m-resolution shaded DEM of upper Monterey Canyon with high, northeasterly illumination angle and 5× vertical exaggeration. (A) View position and direction for Figure 11. (B) Mouth of Elkhorn Slough. (C) Site where dredge material was placed in March 2003. (D) Northern breakwater of the Moss Landing Harbor mouth. (E) 20-m-tall terrace. (F) Head of large complex slump. Arrows with values show partitioned annual sediment load potentially entering the canyon head. Sediment from the north is from Best and Griggs (1991) as modified by Eittrheim (2002b). Sediment from Harbor Mouth is from estimates of estuary erosion by Dean (2003) and Brantner (2001). Sediment from the south is from Dingler et al. (1985).

surface processes of Monterey Bay and its submarine canyon (e.g., Greene, 1990; Greene et al., 2002; Eittrheim et al., 2002a). Additional studies have documented active slumps, turbidity currents, and canyon-axis “flushing events” affecting the Monterey Canyon head (Greene, 1990; Greene and Hicks, 1990; Garfield et al., 1994; Okey, 1997; Greene et al., 2002; Eittrheim et al., 2002b; Paull et al., 2003, 2005; Xu et al., 2004). These studies show that the prevalent canyon-shaping processes include transform faulting, slumping, slump-controlled meanders, fault-controlled meanders, and sediment-gravity flows. Despite these efforts, relatively little is known about sediment transport

frequency and processes or the rates of morphologic change in the canyon. It is unclear whether short-term processes, such as tidal flow and frequent sediment-gravity flows, or less-frequent, but higher magnitude, processes are most important for transporting the annual sediment budget through the upper canyon.

Based upon recent studies, over 300,000 m³/yr of sediment is delivered to the canyon head by northward and southward littoral transport of sand sourced in rivers, coastal erosion, and material eroded from the enlarging Elkhorn Slough (Dingler et al., 1985; Best and Griggs, 1991; Mitts, 2003; Dean, 2003). Although studies of sand petrology have established local water-

sheds as the chief canyon sediment source (Mitts, 2003), the coastal sediment budget remains only loosely approximated (Best and Griggs, 1991). The volume of littoral sediment that bypasses the canyon head along the beach is undocumented as well.

Little is known about the degree to which upper Monterey Canyon stores, transports, or adds to the sediment volume delivered to the head (Paull et al., 2003, 2005; Xu et al., 2004). Based upon a longitudinal profile, Paull et al. (2005) speculate that the upper canyon has been aggrading rather than transporting all the sediment supplied to it. Canyon wall morphology indicates that slumping provides

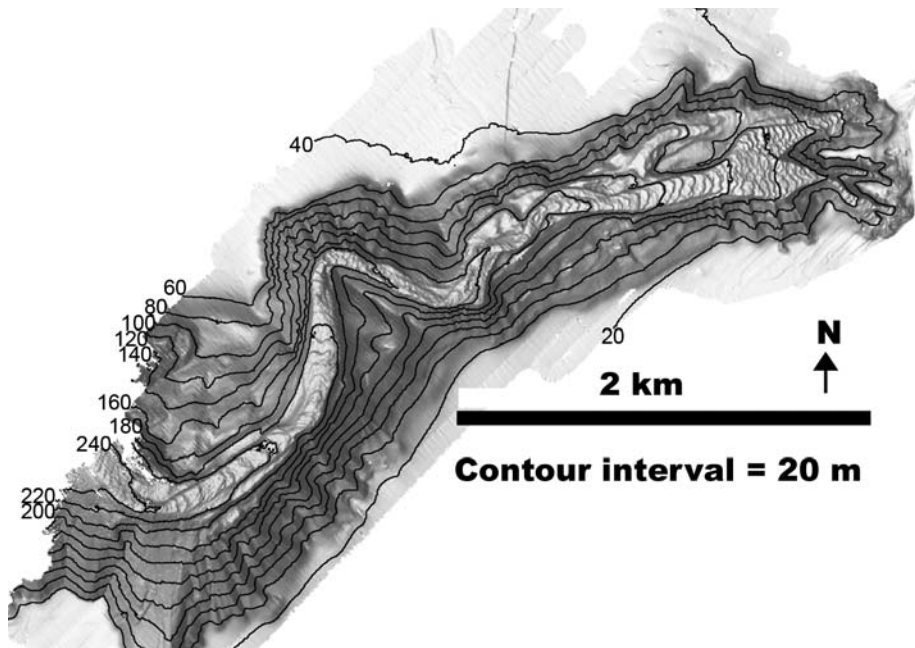


Figure 3. Bathymetric contours plotted on 2003 DEM. The 130 m isobath approximates the 18 ka paleoshoreline at the most recent eustatic sea level lowstand (Pinter and Gardner, 1989).

additional material to the canyon axis on a less regular but sometimes massive scale (e.g., Greene et al., 2002). Very recent slumping has been documented in the walls of the canyon head through serial observations spanning the time of the 1989 Loma Prieta earthquake (Greene and Hicks, 1990; Okey, 1997). However, sand composition in the canyon axis has not been significantly influenced by recent canyon wall sources (Mitts, 2003). Although gullies and sediment chutes are present in the canyon walls, past studies have not determined if they are relict or active features.

Sediment gravity flows have been documented in Monterey Canyon. Okey (1997) noted that in each fall season of a three year study, sediment stored near the Monterey Canyon head suddenly moved down canyon in response to a threshold in ocean surface energy. A few researchers have reported similar events in the heads of submarine canyons, using the term “flushing event” to describe the process (e.g., Shepard and Marshall, 1973; Okey, 1997). The source of the sediment flushed from the head of Monterey Canyon includes the longshore drift, sediment deposited from river floods (Eittrheim et al., 2002b; Mitts, 2003), sediment dredged from the Moss Landing Harbor (e.g., MEC Analytical Systems, Inc., 2003), and sediment eroded from the enlarging Elkhorn Slough estuary (Fig. 1; Brantner, 2001; Dean, 2003). “Flushing events” are clearly the

initiation of sediment gravity flows that periodically move sediment from the shelf-canyon break to deeper water. These sediment-gravity flows are apparently triggered by meteorological events that destabilize sediment stored near the canyon head (Okey, 1997; Paull et al., 2002; Xu et al., 2004), but the details of canyon-head sediment storage and the mechanics of the sediment transport during flushing events are not well established.

This paper explores some of the long-term and more frequent processes shaping the upper Monterey Canyon based upon geomorphic interpretations of recently acquired high-resolution serial bathymetric data and derivative digital elevation models (DEMs). Comparison of three high-resolution DEMs shows the changes in the head and upper 4 km of the canyon during both a 6 month and 24 h period. We present evidence that relatively small-scale, but frequent, processes may be very important in shaping the morphology of the upper 4 km of the canyon, and we quantify the semiannual erosion and deposition rates within the upper canyon. Using serial bathymetric changes, we propose a conceptual model describing the perianual build-up and mass wasting of a sediment wedge at the canyon head. We also present a simple sequence of cutting and filling that has shaped upper Monterey Canyon. Lastly, we comment on the geomorphic effects of placing harbor dredge material near the canyon head.

Geologic Setting

Monterey Canyon extends from the mouth of Moss Landing Harbor at least 90 km offshore to over 3 km depth (Fig. 1). The data and results presented in this paper are restricted to the upper 4 km of the canyon between water depths of 10 and 250 m (Figs. 2 and 3).

The upper canyon occupies the Salinian structural block, between the San Andreas and Palo Colorado–San Gregorio fault zones of the North American–Pacific plate boundary (Greene and Hicks, 1990). Vertical motion of the Salinian block has led to a complex canyon history, with multiple episodes of cutting, widening, and filling starting before 10 Ma (Greene and Hicks, 1990). The most recent canyon cutting occurred in Quaternary time if Wagner et al. (2002) are correct in mapping the Quaternary Aromas Sand, in the uppermost reach of the canyon.

The canyon walls are draped by fine-grained marine sediment (Paull et al., 2005) and are dissected by gullies and landslide features. The canyon floor contains terraces (D in Fig. 4) that bound a dynamic axial channel (E in Fig. 4) that transports fine- to medium-grained beach sand and gravel entering the canyon head (Paull et al., 2005; Mitts, 2003).

DATA ACQUISITION, PROCESSING, AND ANALYSIS

Three hydrographic surveys of the upper portion of Monterey Canyon were conducted using a pole-mounted Reson 8101 244 kHz multibeam sonar on the 27 ft Research Vessel *MacGinitie*. Position was recorded by a Trimble 4700 global positioning system (GPS) with differential corrections provided by a Trimble ProBeacon receiver for a survey on 30 September 2002. A Trimble 5700 real time kinematic (RTK) system provided high-precision positioning for surveys on 25 and 26 March 2003.

The areas mapped in 2002 and 2003 were executed using the same survey line files. An Applanix heading and motion sensor with 0.02° precision corrected for ship motion. An Applied Microsystems Limited Sound Velocity Plus sound velocity profiler was deployed for later adjustment of depth soundings. The wind conditions for all three surveys were relatively calm with flat seas. The multibeam sonar collected bathymetric data across 150° of swath coverage, using 101 1.5° × 1.5° beams. All raw data were logged using a Triton–Elics International Isis Sonar data acquisition system. Survey data files were filtered and cleaned using Caris Hips software. Shoal-biased bathymetry data sets exported from Caris Hips with 2 m horizontal

resolution were examined in Interactive Visualization Systems Fledermaus software for further cleaning, geomorphic analysis, and for exporting grids and geotiffs to ArcMap GIS software for analysis of georeferenced serial images. Resolution of the bathymetry data was such that landscape features and differences on the order of 0.2 m vertical and 3.0 m horizontal were clearly discernable. Data were rigorously edited by hand for spurious points and smoothed and gridded to a 3 m interval to minimize data gaps in the final xyz export.

Accuracy and precision are a function of positioning and attitude measurement errors, timing errors, water depth, tidal correction, and the water sound velocity profile. Errors caused by sensor misalignment, sensor inaccuracy, and timing issues were minimized through standard hydrographic survey patch-test calibration methods performed using sewer outfall pipeline of the nearby city of Marina as a benchmark before each survey. Tidal correction was performed using NOAA-predicted tide values for Monterey Bay for the 2002 survey in which differentially-corrected GPS positioning was used, while the 2003 surveys utilized high-precision three-dimensional RTK positioning that allowed soundings to be referenced to a true vertical datum rather than the water surface, removing the influence of tide from the equation. Predicted tide values used for tidal correction in 2002 agreed with NOAA tide-gauge data, unavailable at the time of the survey, to within 10 cm (mean error \pm SD = 0.05 ± 0.02 m) over the time period of the survey. Measured tidal variation using RTK positioning in 2003 also closely agreed with the observed tide-gauge data (mean error = 0.10 ± 0.04 m). We found that tidal corrections from RTK positioning were more accurate during this sampling period than using predicted tides, which deviated further from the observed values (mean error = 0.60 ± 0.06 m). At least one water column sound velocity profile was collected on each sampling day for use in correcting sounding solutions for sound velocity variation.

Because the analyses performed in this study required comparison of serial DEMs of seafloor morphology, care was taken to ensure that the data sets were properly georeferenced and in vertical registration with one another. The bathymetric grids were vertically registered by slightly shifting one with respect to the other until elevation differences were minimized on flat, stable surfaces that likely remained unchanged between surveys. Between-survey precision of the DEMs was then evaluated using known anthropogenic and natural landmarks that were (1) visible in both the 2002 and 2003 surface models, and (2) unlikely to move or

change over time. For example, the mapped location of the shallowest point at the Duke Energy electrical generating plant cooling outfall shifted only 3.29 m horizontally and 0.47 m vertically between the 2002 and 2003 DEMs. Precision was similar for another landmark, the defunct National Refractories water intake pipe (4.32 m horizontal, 0.51 m vertical). The horizontal error was judged to be relatively small compared to the largest potential sources of error in the overall error budget and was deemed acceptable because it was on the order of one pixel in the horizontal dimension.

The six-month canyon-floor sediment budget was calculated in ArcMap 8.2 by subtracting the bathymetry of the 2003 DEM from the 2002 DEM to determine the net bathymetric change in each pixel. The net vertical differences in each 3×3 m pixel were multiplied by the pixel area (9 m^2) and added to arrive at the net volume difference in specific areas of the canyon. To greatly reduce the chance of including “noise” in our calculations, we only included pixels showing net vertical changes of greater than ± 1 m. Our exclusive use of those high-value pixels has two implications. First, our estimates of bathymetric and sediment-volume changes are underestimates if large regions of the canyon had depth changes of less than ± 1 m in depth. Second, we would overestimate erosion if local erosion, much greater than 1 m, liberated sediment that was redeposited onto a broader area at a thickness less than 1 m. The bathymetric changes presented here include error estimates calculated by multiplying the between-grid depth precision (± 0.5 m) by the sum of the areas of the pixels used in the calculation of bathymetric change (i.e., those with greater than 1 m differences).

RESULTS

General Morphology

Within the study area, the canyon floor width ranges from 30 m to 440 m. The most constricted point is at the “narrows,” the apex of a tight canyon meander, whereas the broadest channel segment is near the canyon head where four steep tributaries meet the canyon floor (Fig. 2). The canyon has an average top width of ~ 1000 m. The top width increases rapidly down canyon. An obvious break in slope between the upper canyon wall and the continental shelf defines the top-width measurement (Fig. 4). The canyon walls have a maximum relief of 190 m (Fig. 3) and are marked by slump scars and gullies (Fig. 5). The sinuosity of the axial channel is 1.2 along a channel length of 5150 m. Canyon tributary heads have channel gradients of $\sim 7^\circ$; the channel floor gradient below the tributar-

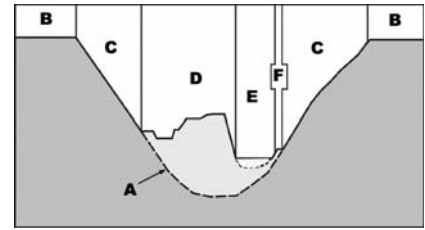


Figure 4. Speculative, schematic cross section of upper Monterey Canyon illustrating general geomorphic zones. Figure represents a cross section ~ 900 m down canyon from the head. Labeled regions are more fully described in text. Arrow A indicates speculative buried contact between Aromas Sands (dark gray; Wagner et al., 2002) and canyon fill sequences (light gray and stipple). (B) Transition from canyon walls to continental shelf. (C) Canyon walls. (D) Terraces developed in older canyon fill. (E) Axial channel carries modern gravelly sand bedload. (F) Minor terraces composed of unconsolidated sand; these terraces are short-lived features associated with subannual incision of axial channel through recent bedload material. “Canyon floor” in text includes regions D, E, F.

ies is $\sim 1.5^\circ$. Sand waves and complex terraces dominate the canyon floor (Figs. 2 and 5).

Canyon Head

Monterey Canyon has a 700-m-wide, amphitheater-shaped, compound head composed of four smaller tributary heads (Fig. 2). The tributaries are 300-m-long, high-gradient, steep-walled canyons. There are two northern heads and two southern heads separated by a 150-m-wide, 500-m-long ridge probably composed of older canyon fill (Wagner et al., 2002). The northernmost head terminates north of the Moss Landing Harbor breakwater (point D in Fig. 2). The breakwater terminates at the shelf-canyon break (Fig. 2). The walls of the tributary have minor gullies, and complex, sand waves cover the floor. The wavelength of these bedforms ranges from 20 to 40 m, and the crests are sharply defined with down-canyon asymmetry.

The next head to the south terminates between the breakwaters bounding the mouth of Moss Landing Harbor (Fig. 2). The walls and floor of the tributary are smooth, with muted bedforms near its mouth. During the six month span of the study there was significant sediment storage at the lip of this canyon head (Fig. 6). Close comparison of the 2002 and 2003 bathymetric data shows that a prograding sediment wedge moved the shelf-slope break ~ 10 m seaward in

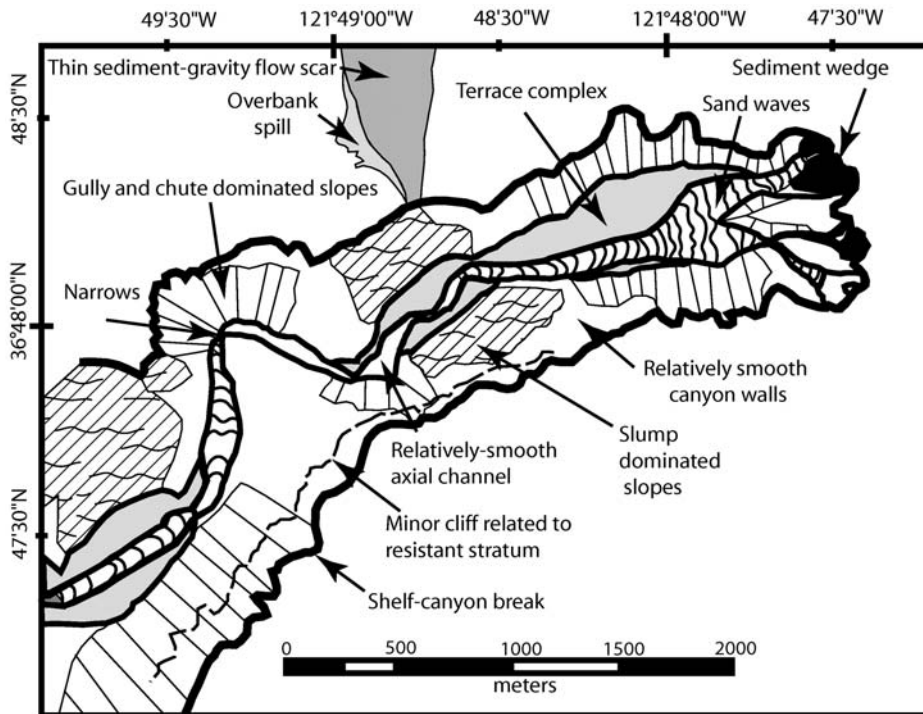


Figure 5. Geomorphic features of upper Monterey Canyon interpreted from Figure 2.

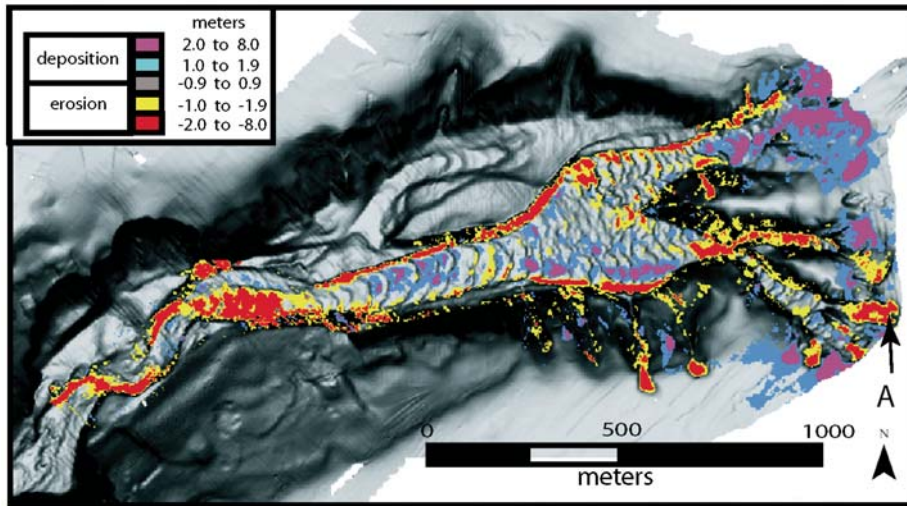


Figure 6. Raster subtraction of March 2003 DEM from September 2002 DEM showing locations of significant net erosion and deposition near the head of Monterey Canyon. Scour is present at outside of intracanyon meander bends. Channel widening is shown by scour along channel floor margin. Gully head extension is evident on southern wall gullies (see Fig. 7). Sediment storage occurred in several of the canyon head tributaries. Arrow points to site A where dredge material was placed in March 2003 and has net erosion of over 2 m. See Figure 2 for location.

this tributary head. The mouth of this tributary hangs slightly above the northernmost tributary channel at an erosional scarp.

The southern two tributary heads terminate 300 m and 500 m south of the southern Moss

Landing Harbor breakwater (point C in Fig. 2). Both of these tributary canyons are strongly V-shaped, with minor gullying in the walls and a narrow ribbon of sediment present along their thalwegs. The sediment along the thalwegs

forms well-defined sand waves with wavelengths from 10 m to 45 m.

Canyon Walls

The canyon walls can be divided into the following geomorphic categories, from most to least abundant: (1) gullies and chute-complexes, (2) relatively smooth walls, and (3) zones with evidence of slumping and/or mildly hummocky slopes indicative of creep (Figs. 2 and 5). Gullies are nearly straight, steep-floored (12° to 20°) sediment conduits with well-developed channel sides, whereas chute complexes are steeper and have branching, straight channels. The chute complex present northwest of the narrows has a slope of 25° and very straight channels that branch upward into a tributary network (Fig. 2). The southeastern canyon wall beginning 500 m downstream from the narrows is creased with many straight, parallel chutes and gullies (Figs. 2 and 5). These features are crosscut by a 20-m-tall canyon floor terrace at their downslope terminations. Two gullies on the south canyon wall located ~500 m from the southern tributary head grew headward ~60 m during the six month period (Fig. 7). A 5-m-tall terrace located at the mouths of the gullies was removed through lateral erosion during the same time period (Fig. 7).

Three sections of canyon wall are dominated by slump and other slope-failure features (Fig. 5). Within each of these reaches there are nested headwall scarps with varying degrees of rounding, suggesting multiple slump events with a range of relative ages. The largest slump complex we imaged is at least 700 m wide, starting ~400 m down canyon from the narrows on the northeast canyon wall (Figs. 2 and 5). The down-canyon edge of the slump lies beyond the western edge of our data (Fig. 2). This slump complex includes a broad, arcuate headwall scarp with well-rounded slopes. The toe of the large slide is bordered by terraces along the axial channel, suggesting that the terrace-forming processes are more recent than the slope failure. Within the main slide body are several minor slump features.

A more sharply defined slide complex is located on the northwestern canyon wall ~600 m up canyon from the narrows (Figs. 2 and 8). At the base of the slide scar there is a stepped terrace that helps define an “intracanyon meander” (Fig. 8; Greene et al., 2002). The intersection of the terrace and the northwestern canyon wall defines a broad canyon wall meander (Fig. 8). The terrace material at the toe of the slump scar lacks the hummocky topography typical of slide deposits.

Canyon Floor

The canyon floor can be divided into two geomorphic regions: (1) an axial channel that contains active sand waves (E in Fig. 4 and Fig. 5), and (2) complex terraces that locally bound the axial channel on both sides of the canyon (D in Fig. 4 and Fig. 5).

One striking feature of these high-resolution images is the sand-wave field on the canyon floor, which previous imagery has not revealed (Fig. 2). In general the sand waves have crescentic to undulating crests, which commonly can be traced for 100 m. The sand waves are strongly asymmetric with slip faces oriented down canyon, indicating a dominant downslope sediment transport direction. Figure 9 illustrates the complete reorganization of sand waves in the six month period and lack of change during the 24-h period. The sand waves imaged in 2002 had wavelengths of 15 m to 50 m, with a dominant wavelength of ~30 m. The sand waves in the main channel had an average wavelength of 36 m and wave height of ~2 m. Along an identical profile through the 2003 data, the waves were more organized and larger with an average wavelength of 46 m and height of between 4 and 5 m (Fig. 10A). In both years, the wavelengths shorten up canyon with increased canyon floor gradient. For example in 2003, the northern tributary had waves with an average length of 26 m and average height of 2–3 m (Fig. 10B). Serial longitudinal profiles of the sand waves over a 24-h period between 24 and 25 March 2003 show no significant change in the sand waves during a full tidal cycle.

Terraces are locally present on both sides of the axial channel (Fig. 5; D in Fig. 4). The terrace complex located in the deepest part of the study area (point E in Fig. 2) includes two terraces with the lower terrace 20 m above the axial channel and the higher terrace 50 m above the axial channel. The lower terrace riser is very straight in map view (Fig. 2). The terrace complex located 1000 m down canyon from the head contains several minor depositional or erosional surfaces and a perched channel that lies above the grade of the modern axial channel. This apparently abandoned channel is cut off from the head tributaries by a 2-m-tall erosional scarp, and its mouth hangs several meters above the axial channel (Figs. 2 and 11).

The six-month canyon-floor sediment budget was calculated by subtracting the bathymetric data collected in 2003 from those collected in 2002. Sediment storage in the tributaries, erosion in meander bends and floor margins, and terrace-forming incision are well defined in the resulting image (Fig. 6). Where intracanyon meanders have formed (Fig. 8), the channel

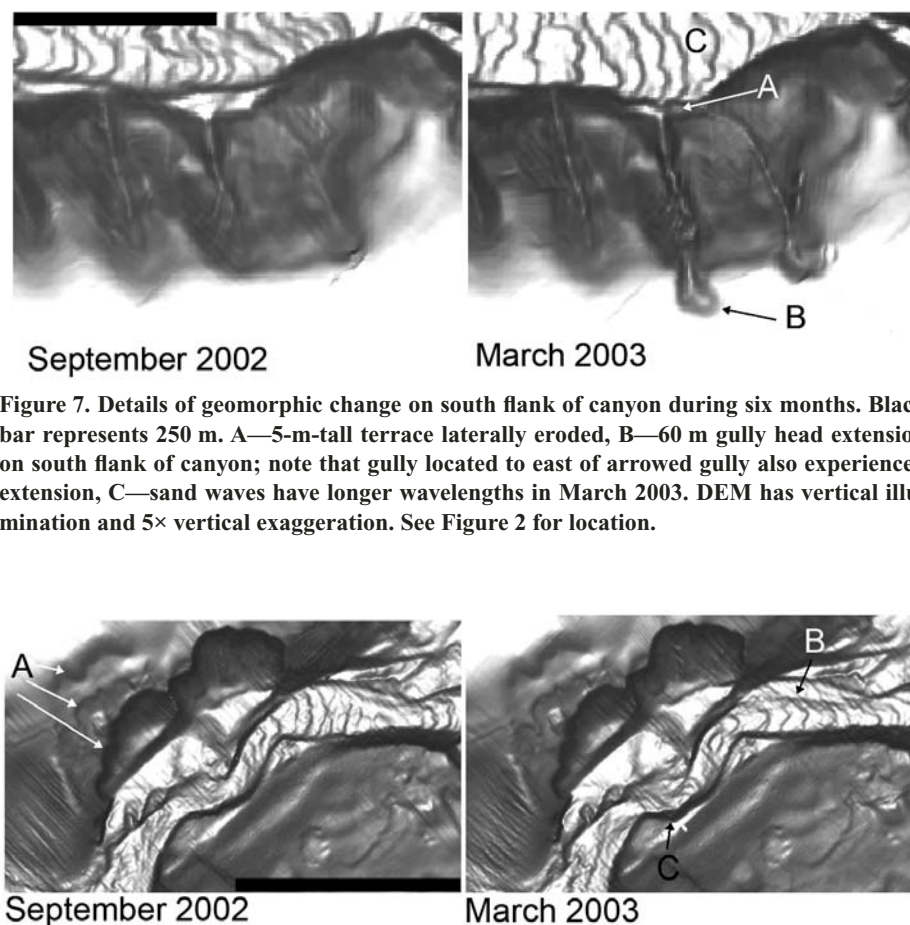


Figure 7. Details of geomorphic change on south flank of canyon during six months. Black bar represents 250 m. A—5-m-tall terrace laterally eroded, B—60 m gully head extension on south flank of canyon; note that gully located to east of arrowed gully also experienced extension, C—sand waves have longer wavelengths in March 2003. DEM has vertical illumination and 5× vertical exaggeration. See Figure 2 for location.

Figure 8. Details of geomorphic detail and change along intracanyon meanders during six months. North is toward top of image, and black bar represents 500 m. A—“nested” headwall scarps in young slumps on northern canyon wall, B—2-m-tall terrace formed by axial-channel incision, C—lateral erosion at outside of bend. NW-SE-oriented “grooves” are noise in bathymetric data. DEM with vertical illumination and 5× vertical exaggeration. See Figure 2 for location and Figure 11 for perspective view.

thalweg shows clear evidence of as much as 4 m of vertical scour at the outsides of the bends (Fig. 6). Overall, erosion of 320,000 m³ (±80,000 m³) of sediment was approximately balanced by 260,000 m³ (±70,000 m³) of sediment deposition during the six month study. The erosion and deposition were concentrated in different regions of the canyon (Fig. 6).

DISCUSSION

Serial, high-resolution shaded relief digital bathymetry models reveal new geomorphic detail in the upper Monterey Canyon. These data foster interpretations of canyon processes and physical evolution with higher spatial and temporal resolution than was previously possible. We speculate here on the short- and long-

term processes influencing the upper Monterey Canyon morphology.

Annual Sediment Budget

The annual sediment budget of Monterey Canyon and the modes of down-canyon sediment transport are difficult to determine and remain poorly documented. We partition the sediment load among canyon head tributaries and discuss the role of canyon processes in modifying the sediment budget passing through the upper canyon.

The northernmost canyon head tributary (point D in Fig. 2) is the southern terminus of a littoral cell extending as far north as the San Francisco Bay (Best and Griggs, 1991). Littoral sediment entering the northern tributary

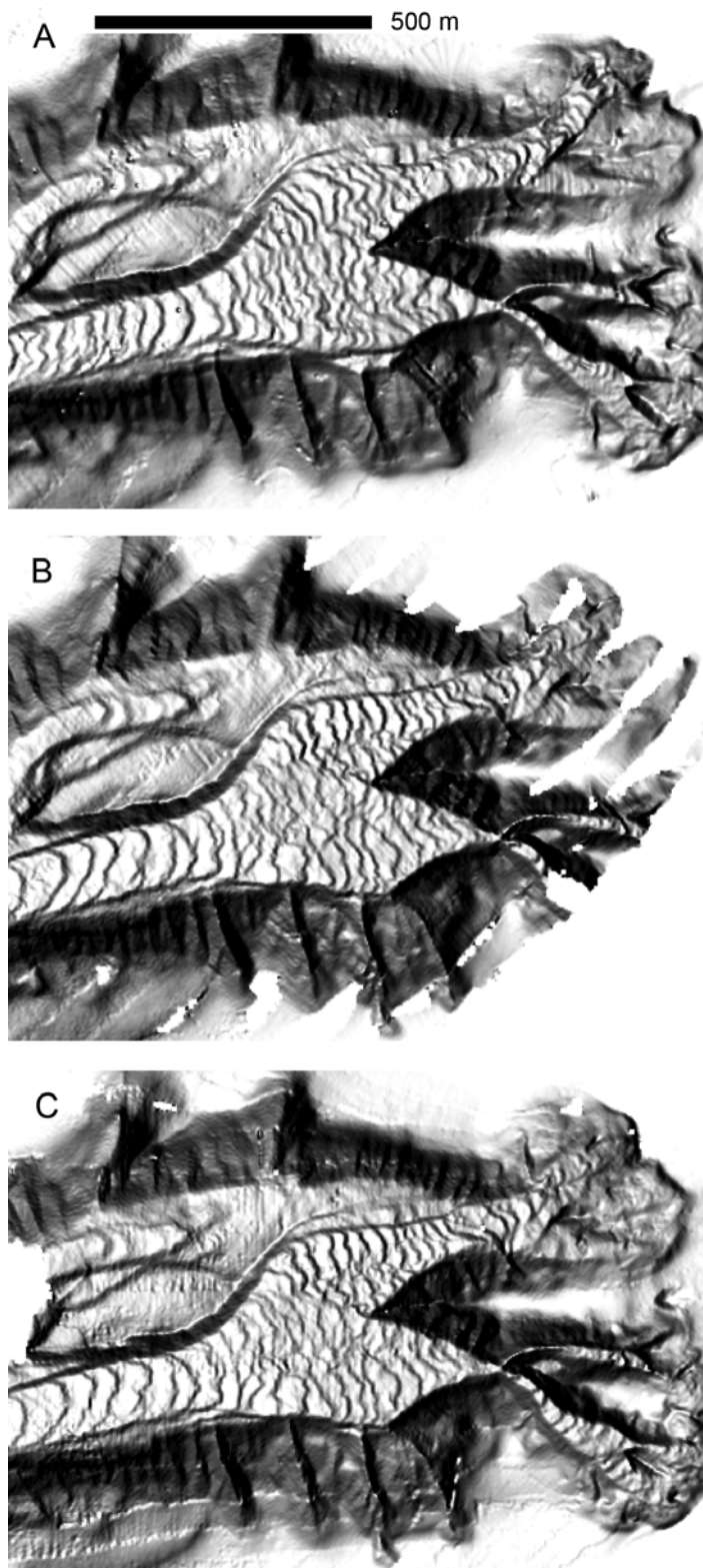


Figure 9. Comparisons of three surveys of the upper canyon. (A) September 2002. (B) 24 March 2003. (C) 25 March 2003.

canyon each year from the north may be as high as 200,000 m³ to 250,000 m³. Eittrheim et al. (2002b) conservatively suggest using the lower limit of 200,000 m³ as an annual average. Because the northern harbor breakwater terminates virtually at the shelf-canyon break (Fig. 2), it is not likely that a significant portion of the southbound littoral drift bypasses the breakwater or the canyon head. Therefore the breakwater may play a significant role in limiting the sand budget of southern Monterey Bay. Previous studies also indicate that significant littoral sediment does not bypass the Monterey Canyon head (Sayles, 1966; Tait and Revenaugh, 1998).

The tributary head terminating between the Moss Landing Harbor breakwaters (Fig. 2) is the seaward extension of Elkhorn Slough, an enlarging coastal estuary. During the six month period, ~73,000 m³ of sediment were naturally deposited in a sediment wedge at the Harbor mouth, while only 4000 m³ were naturally eroded (Fig. 6), leaving a net volume in the wedge of 69,000 m³. This sediment wedge is built from a combination of sediment eroded from Elkhorn Slough, littoral drift from the south, and littoral drift from the north that managed to be carried through the narrow passage between the northern tributary mouth and the end of the northern breakwater (Fig. 2). Although between 56,000 m³ and 86,000 m³ of sediment are annually eroded from Elkhorn Slough (Brantner, 2001; Dean, 2003), it is unclear how much of that sediment enters the canyon head because much of the eroded material is likely to be suspended fine sediment that either bypasses the head or settles in still water of intervening Moss Landing harbor. The sediment temporarily deposited in Moss Landing Harbor commonly reaches the canyon through dredging efforts.

The two southern tributary heads (near point C in Fig. 2) annually receive somewhere between 50,000 m³ and 155,000 m³ of sand-size littoral drift sediment transported northward from seacliff erosion and the mouth of the Salinas River (Dingler et al., 1985; Watson et al., 2003; E. Thornton, 2003, personal commun.). The presence of a 350-m-wide submarine dune field immediately down canyon from these tributaries attests to the energetic transport of sand-sized sediment entering the canyon from the south (Fig. 2). Sediment entering the southern tributaries has locally aggraded the channel in excess of 2 m (Fig. 6). These canyon heads also sporadically receive the sediment dredged from Moss Landing Harbor. Approximately 16,200 m³ of material dredged from the harbor was gradually placed very near the southern canyon heads (point D in Fig. 2) between 6 and 13 March,

ending just 11 days before the 24 March 2003 survey (MEC Analytical Systems, Inc., 2003).

Sand Waves and Canyon Currents

Two canyon processes that can produce the requisite shear force to move the axial channel bedload are tidal currents and sediment gravity flows. The upper reach of Monterey Canyon receives and transports $\sim 300,000 \text{ m}^3/\text{yr}$ of sediment derived from multiple external sources. The material transported as bedload in the axial channel is fine- to medium-grained sand with a variable amount of gravel (Table 1 and Fig. 12; Mitts, 2003; Paull et al., 2005).

Tidal Currents

Although tidal currents along the floor of Monterey Canyon twice daily exceed the velocity required to move the sand-sized bedload in the axial channel, the currents are oriented against the slip faces of the sand waves (Petruncio et al., 1998; Rosenfield et al., 1999). These tidal currents are therefore not responsible for developing the large bedforms associated with large-scale, down-canyon sediment transport.

Sediment-Gravity Flows

Several studies have detailed sediment-gravity flows in Monterey Canyon (e.g., Paull et al., 2003; Garfield et al., 1994; Xu et al., 2004). Xu et al. (2004) reported that there were two significant turbidity currents, likely sourced in upper Monterey Canyon, that occurred during the six months between our surveys. The first occurred on 20 December 2002, coincident with very high surf and high terrestrial stream flow (Xu et al., 2004). The maximum velocity at the moored instruments was 190 cm/s, more than enough velocity to move ambient sand in the axial channel as well as any suspended load in the current. The second turbidity current occurred on 14 March 2002, following by three days the placement of 16,200 m^3 of Moss Landing Harbor dredge sediment at the southern head of the canyon (MEC Analytical Systems, Inc., 2003). There was greater than 2 m of net erosion at the dredge placement site between the 2002 and 2003 surveys rather than the expected net deposition (Fig. 6). It is possible that the loose dredge material slid downslope as the trigger for the 14 March turbidity current recorded by Xu et al. (2004). Alternatively, the dredged material may have washed away as suspended load in littoral currents.

Our data indicate that strong down-canyon currents are capable of significant geomorphic work and sediment transport. The elimination of tidal currents as a mechanism and the coincidental turbidity currents measured by Xu et al. (2004) lead us to conclude that sediment

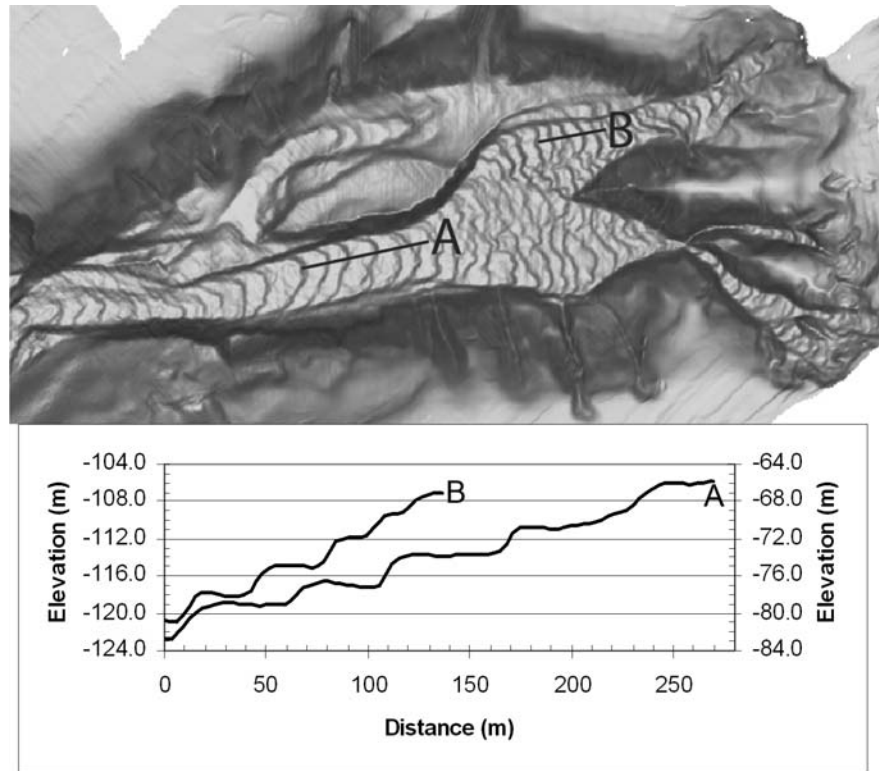


Figure 10. (A) Profile of sand waves in trunk channel on 24 March 2003. Left-hand elevation scale applies to profile A. (B) Profile of sand waves in northern tributary channel on 24 and 25 March 2003. Right-hand elevation scale applies to profile B.

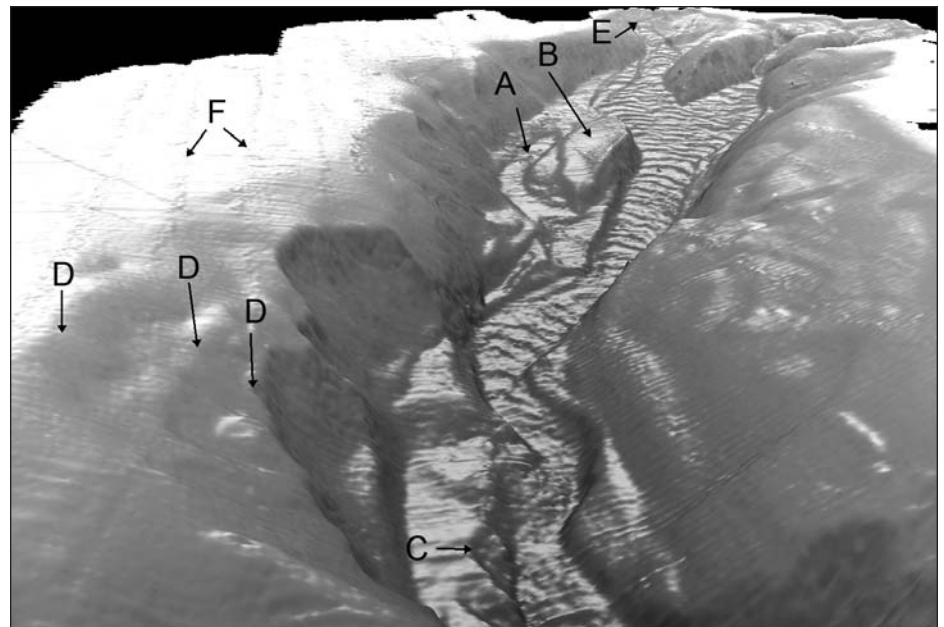


Figure 11. Perspective view toward head of Monterey Canyon. View shows axial sand waves, intracanyon meanders, multiple slumps, and complex terraces. Vertical illumination and 5 \times vertical exaggeration. Bathymetric data from September 2002. A—remnant meander, B—complex 25-m-tall terrace, C—minor slump on outside of modern meander, D—nested headwall scarps on northern canyon wall (see Fig. 8 for map view), E—northern tributary head, F—parallel lines are data acquisition artifacts.

TABLE 1. SEDIMENT GRAIN SIZE IN UPPER MONTEREY CANYON

Symbol [†]	Geomorphic setting [‡]	Location description [‡]	Depth (m) [§]	Core length (cm) [§]	Mud (%) [§]	Sand + silt (%) [§]	Gravel (%) [§]	Vibracore sample [§]
35	Axial channel	100-m-wide, 70-m-long, low amplitude crescentic sand waves	201	165	0	100	0	V1905-VC-35
36	Axial channel	Same as above	202	146	0	100	0	V1906-VC-36
55	Axial channel	Steep gradient and shorter wavelength	86	216	0	100	0	V1947-VC-55
85	Axial channel	Complex floor in intracanyon meanders	151	57	0	52	48	V2129-VC-85
86	Axial channel	Same as above	150	197	0	53	47	V2130-VC-86
87	Terrace	Smooth surface	135	239	85	15	0	V2131-VC-87

[†]Plotted on Figure 12.
[‡]Present in March 2003 bathymetry.
[§]Data from Paull et al. (2005).

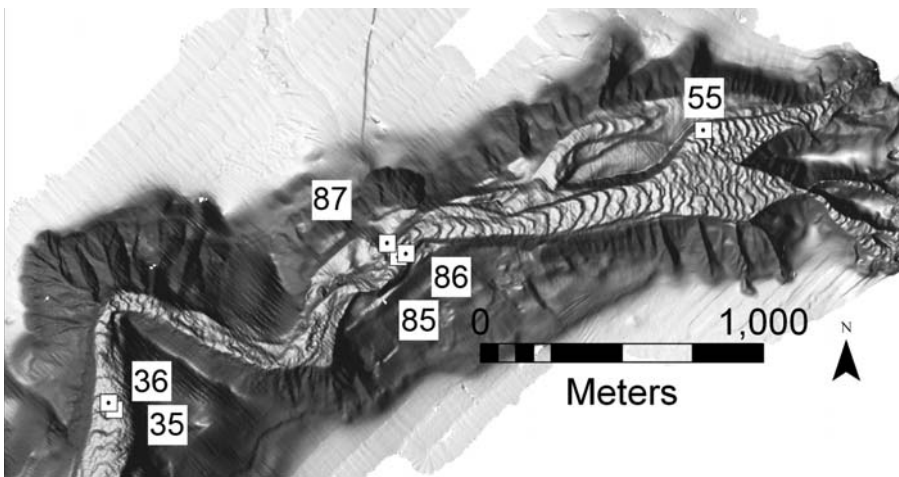


Figure 12. Map of canyon bottom sediment samples shows that channel axis is chiefly sand, whereas terrace material is mud. Small white boxes with black dots are vibracore sample localities published in Paull et al. (2005). Larger, numbered boxes are labels for the core localities that refer to sediment data in Table 1.

gravity flows are the chief processes transporting sand and maintaining sand waves in upper Monterey Canyon.

Sedimentary Cycles at the Monterey Canyon Head

Shepard (1981) suggested that small but frequent turbidity currents might be the dominant sediment transport mechanism along modern submarine canyons. We propose that Monterey Canyon undergoes a subannual cycle of sediment deposition at the lip of the canyon followed by slope failure when a critical combination of variables exceeds the strength of the sediment wedge. When the slope fails, the sediment is transported by some combination of sediment gravity flow processes. The reports of resuspended sediment visible at the sea surface (“flushing event;” e.g.,

Okey, 1997) suggest that large-scale mixing occurs during the initiation of sediment transport, probably leading to a turbidity current.

During the six month study, a prograding sediment wedge moved the shelf-slope break ~10 m seaward in the tributary located at the mouth of Moss Landing Harbor. It is unclear if the ~73,000 m³ of sediment in the sediment wedge gradually accumulated during the entire six months or if the canyon experienced one or more interim progradation-slope failure cycles during the study period. Evidence supporting at least one sediment-gravity flow sourced in the canyon head is the complete reorganization of the sand waves in the bottom of the canyon and significant amount of channel scour during the same time span (Figs. 6 and 9).

Environmental conditions that could trigger slope failure of the sedimentary wedge are

regularly achieved at the lip of Monterey Canyon. Slope failure at the lip of Monterey Canyon probably occurs when storm waves destabilize a growing sediment wedge that has the proper combination of sediment thickness, grain size distribution, and seaward slope. Storm waves of only 2.5 m in height were able to destabilize the 15-m-deep Huanghe Delta on a slope of less than 1% (Prior et al., 1989). Conditions for slope failure are far greater at the Monterey Canyon where the sediment wedge lies at ~10 m depth, the seaward slope on the sediment wedge is greater than 25%, and winter waves regularly exceed 3 m. During the six-month study period there were five significant storms, including a storm with 8.5 m seas (Renard, 2003).

The combination of anecdotal evidence (e.g., Okey 1997), remotely deployed instruments (Garfield et al., 1994; Paull et al., 2003; Xu et al., 2004), and serial bathymetry demonstrates that Monterey Canyon actively transports sand and gravel and does so through subannual sediment-gravity flows, including turbidity currents.

Geomorphic Processes and Canyon Evolution

The detailed bathymetric images allow us to propose a two-dimensional, three-phase evolutionary model for the upper Monterey Canyon (Fig. 13). We emphasize that the canyon has very likely had a more complex history (e.g., Greene and Hicks, 1990), but the model includes the minimum, large-scale, defensible steps that are required to develop the canyon cross section that we see today near the tall terrace complex (point B in Fig. 11).

Phase one is large-scale incision into pre-existing landscape and substrate that began at least 10 million years ago (Greene and Hicks, 1990). The canyon walls, above the canyon floor terraces, are composed of weakly consolidated Pleistocene Aromas Sand (Wagner et al., 2002) or a veneer of mud over that formation (Paull et al., 2005). By analogy with modern terrestrial watershed systems, the canyon underwent repeated cycles of downcutting, widening, and partial filling that resulted in excavation of a deep, broad canyon.

Phase two is partial filling of the canyon (Fig. 13). These deposits compose the modern terraces that stand tall above the modern axial channel; therefore, the canyon filled at least as high as the top of the highest local terraces. Vibracore sample 87 (Fig. 12) shows that at least one of the terraces comprises interstratified sand and silt (Mitts, 2003), with mud being the dominant component (Table 1; Paull et al., 2005). The stratified fine-grained deposits in the terrace indicate deposition in a relatively low-energy environment with reduced input of

coarse clastic sediment. These deposits may have resulted from rising sea level or damming by down-canyon landslides. Landslide dams have been interpreted much farther down canyon as well (Greene et al., 2002). It is possible that the fill material itself is landslide debris from the canyon walls; however, the terraces have relatively flat, low-gradient surfaces suggestive of in situ deposition, in contrast to the more disturbed landforms associated with submarine landslide deposits elsewhere (e.g., Greene et al., 2002). Lastly, if the terraces were landslide debris from the Aromas Sand composing the canyon wall, they would be composed of nearly 100% well-sorted Aeolian and fluvial sand.

Phase three is incision and advection of the previously deposited fill material as vigorous currents locally carved a series of axial channels in the canyon floor (Fig. 13). Phase 3A (Fig. 13) shows the formation of the now-abandoned channel located north of the tall terrace (point A in Fig. 11). That channel has relict, low-amplitude sand waves, indicating that it was once providing the same function as the modern axial channel. Phase 3B (Fig. 13) shows the incision of the modern axial channel. The incision beheaded the channel formed in phase 3A time, pirating the sand bedload to the south side of the canyon floor. Sand waves located in the abandoned channel are not as sharply defined as the waves in the axial channel but are clearly not deeply buried by Holocene mud, suggesting a relatively recent age for downcutting of the abandoned channel and the modern axial channel. In total 25 m of incision is recorded on the south side of the terrace (Fig. 11). The canyon floor along the narrows has no fill terraces, so either the phase-two fill never accumulated there to great depth, or phase-three advection is nearly complete. Conservation of mass likely accelerates sediment gravity flows in relatively narrow reaches of submarine canyons. The resulting higher velocity in the narrows would favor erosion over deposition.

Evidence for Continued Phase-Three Erosion

Both erosion and sediment deposition play a significant role in the subannual evolution of the canyon floor, but we suggest that phase-three fill excavation is the dominant canyon process today. The young age of some terraces is demonstrated in serial images taken six months apart showing lateral erosion that removes the edges of terraces and local downcutting that produces new terraces (e.g., Figs. 6, 7, and 8).

Widening of the axial channel can potentially destabilize the canyon walls through undercutting. Lateral erosion is apparent in Figure 7, where a terrace was removed during the six month study. Removal of that terrace may have initiated a headcut that rapidly migrated up slope

leading to local gully head extension (Fig. 7). The Aromas Sand is poorly consolidated, so headcut migration may proceed rapidly. The intracanyon meanders show very concentrated scour at the outsides of bends (Fig. 6). Minor headwall scarps are present where the scour is deep along the intracanyon meanders (point C in Fig. 11), suggesting both that the terrace was undercut and that the slump toe was advected down gradient. The obvious concentration of shear stress on the margins of the axial channel is evidence supporting the contention of Greene et al. (2002) that canyon wall undercutting is a modern mechanism for destabilizing slopes and triggering slumps in submarine canyons.

Chutes present in the outer wall of the bend of the narrows are also indicative of canyon widening (Fig. 2). The sharpness of the ridges dividing the chute channels northwest of the narrows indicates that the chute system is not relict but instead is a frequent pathway for debris sourced through headward extension of the chute system into the continental shelf.

CONCLUSIONS

Our interpretations support and build upon those of Paull et al. (2005), who document the canyon as a very active sediment transport system, despite the modern high eustatic sea level. The floor of Monterey Canyon has experienced a complex Holocene history of filling and erosion. Lateral erosion and vertical incision have been the most recent canyon-shaping processes. The dominant process in the recent past has been downcutting of the axial channel, incrementally increasing the relief on the canyon walls. The formation of submarine canyon terraces is analogous to fluvial terrace formation; channel incision through older valley fill leaves the axial channel lower in elevation, separated from a flat bench by a tall scarp (Fig. 11). Canyon-widening processes are expressed as slumps, gullies, and chutes. Relatively recent events include channel margin erosion and gully enlargement (Figs. 6 and 7).

In this report we speculate that the subannual terrace-building incision shown in the data is part of a monotonic trend of canyon-fill advection and that the sediment build-up at the canyon head is part of a perianual cycle of sediment storage and down-canyon transport. As support for monotonic advection of terrace fill, we point to the present large height of the terrace scarps, which may record the cumulative result of many years of incremental active-channel incision. Further, the relative youth of the abandoned channel (point A in Fig. 11) indicates recent net downcutting of the axial channel, beyond the amount detected in the six month comparison.

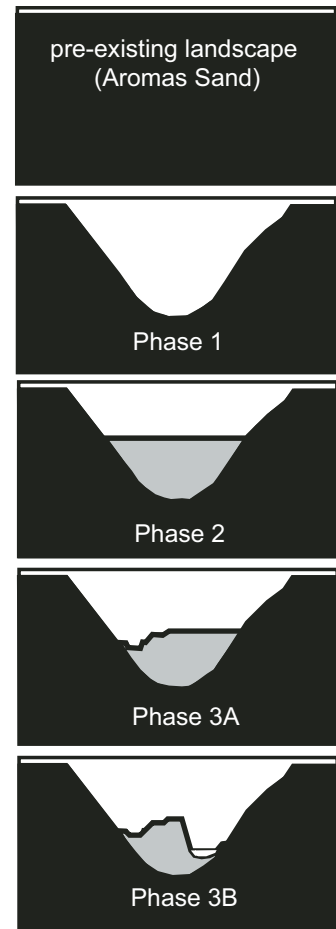


Figure 13. Speculative three-phase evolution model for upper Monterey Canyon.

Both of these speculative points can be tested with future high-precision hydrographic surveys of the upper Monterey Canyon.

ACKNOWLEDGMENTS

This project was supported by the Monterey Bay National Marine Sanctuary SIMoN program, the NOAA CICEET funding program, and NOAA-COTS CICORE. We thank the staff and students at the Seafloor Mapping Lab of California State University Monterey Bay for technical support during and following the cruises of the R/V MacGinitie. Thorough reviews by Charlie Paull, Gary Greene, and two anonymous reviewers greatly improved the focus of the paper. Edward Thornton, John Oliver, and Leslie Turrini-Smith provided comments on an early draft. Leslie Rosenfeld and Jingping Xu guided us toward recent measurements of strong currents and internal tides in Monterey Canyon.

REFERENCES CITED

- Best, T.C., and Griggs, G.B., 1991, A sediment budget for the Santa Cruz littoral cell, California, in Osborne, R.H., ed., From Shoreline to Abyss: Contributions in Marine Geology in Honor of Francis Parker Shepard: Society for Sedimentary Geology Special Publication 46, p. 35–50.

- Brantner, J.E., 2001, Rates of erosion and habitat loss in the Elkhorn Slough [B.S. thesis]: Monterey Bay, California State University, 22 p.
- Dean, E.W., 2003, Tidal Scour in Elkhorn Slough, California: A Bathymetric Analysis [B.S. thesis]: Monterey Bay, California State University, 125 p.
- Dingler, J.R., Laband, B.L., and Anima, R.J., 1985, Geomorphology framework report, Monterey Bay: Los Angeles, U.S. Army Corps of Engineers Report CCSTWS 85-2, 108 p.
- Eittrreim, S.L., Anima, R.J., and Stevenson, A.J., 2002a, Seafloor geology of the Monterey Bay area continental shelf: *Marine Geology*, v. 181, p. 3–34.
- Eittrreim, S.L., Xu, J.P., Noble, M., and Edwards, B., 2002b, Toward a sediment budget for the Santa Cruz shelf: *Marine Geology*, v. 181, p. 235–248.
- Garfield, N., Rago, T.A., Schnebele, K.J., and Collins, C.A., 1994, Evidence of a turbidity current in Monterey Submarine Canyon associated with the 1989 Loma Prieta earthquake: *Continental Shelf Research*, v. 14, p. 673–686.
- Greene, H.G., 1990, Regional Tectonics and structural evolution of the Monterey Bay region, Central California, in Garrison, R.E., Greene, H.G., Hicks, K.R., Weber, G.E., and Wright, T.L., eds., *Geology and Tectonics of the Central California Coastal Region, San Francisco to Monterey*: Pacific Section of American Association of Petroleum Geologists Volume and Guidebook, p. 31–56.
- Greene, H.G., and Hicks, K.R., 1990, Ascension-Monterey canyon systems: History and development, in Garrison, R.E., Greene, H.G., Hicks, K.R., Weber, G.E., and Wright, T.L., eds., *Geology and Tectonics of the Central California Coastal Region, San Francisco to Monterey*: Pacific Section of American Association of Petroleum Geologists Volume and Guidebook, p. 229–250.
- Greene, H.G., Maher, N., and Paull, C.K., 2002, Physiography of the Monterey Bay Marine Sanctuary and implications about continental margin development, in Eittrreim, S.A., and Noble, M., eds., Special Issue: Seafloor geology and natural environments of the Monterey Bay National Marine Sanctuary: *Marine Geology*, v. 181, p. 55–84.
- M.E.C. Analytical Systems, Inc., 2003, Dredge Operations and Monitoring Report: Tiburon, California, Moss Landing Harbor Final Report, 5 p.
- Mitts, P.J., 2003, Deposition and provenance of modern coarse sediment in Monterey Submarine Canyon [M.S. thesis]: Moss Landing Marine Laboratories, San Jose State University, California, 186 p.
- Okey, T.A., 1997, Sediment flushing observations, earthquake slumping, and benthic community changes in Monterey Canyon Head: *Continental Shelf Research*, v. 17, p. 877–897.
- Paull, C.K., Greene, H.G., Ussler, W., III, and Mitts, P.J., 2002, Pesticides as tracers of sediment transport through Monterey Canyon: *Geo-Marine Letters*, v. 22, p. 121–126.
- Paull, C.K., Ussler, W., III, Greene, H.G., Keaten, R., Mitts, P., and Barry, J., 2003, Caught in the act: The 20 December 2001 gravity flow event in Monterey Canyon: *Geo-Marine Letters*, v. 22, p. 227–232.
- Paull, C.K., Ussler, W., III, Keaten, R., Mitts, P., and Greene, H.G., 2005, Trail of sand in upper Monterey Canyon: *Geological Society of America Bulletin* (in press).
- Petruncio, E.T., Rosenfeld, L.K., and Paduan, J.D., 1998, Observations of the internal tide in Monterey Canyon: *Journal of Physical Oceanography*, v. 28, p. 1873–1903.
- Pinter, N., and Gardner, T.W., 1989, Construction of a polynomial model of sea level: Estimating paleo-sea level continuously through time: *Geology*, v. 17, p. 295–298.
- Prior, D.B., Suhayda, J.N., Lu, N.-Z., Hornhold, G.H., Wiseman, W.J., Wright, L.D., and Yang, Z.-S., 1989, Storm wave reactivation of a submarine landslide: *Nature*, v. 341, p. 47–50.
- Renard, R., 2003, National Weather Service Climatological Station, Monterey, California: http://www.weather.nps.navy.mil/renard_wx/ (viewed on August 7, 2003).
- Rosenfeld, L.K., Paduan, J.D., Petruncio, E.T., and Goncalves, J.E., 1999, Numerical simulations and observation of the internal tide in a submarine canyon: Honolulu, 11th 'Aha Huliko'a Hawaiian Winter Workshop, p. 63–71.
- Sayles, F.L., 1966, A reconnaissance heavy mineral study of Monterey Bay beach sediment, Report HEL 2-15, Hydraulic Engineering Laboratory [M.S. thesis]: Berkeley, California, University of California, 105 p.
- Shepard, F.P., 1981, Submarine canyons: Multiple causes and long-time persistence: *American Association of Petroleum Geologists Bulletin*, v. 65, p. 1062–1077.
- Shepard, F.P., and Marshall, N.F., 1973, Storm-generated current in La Jolla Submarine Canyon, California: *Marine Geology*, v. 15, p. M19–M24.
- Tait, J.F., and Revenaugh, J., 1998, Source-transport inversion: An application of geophysical inverse theory to sediment transport in Monterey Bay, California: *Journal of Geophysical Research*, v. 103, p. 1275–1283.
- Wagner, D.L., Greene, H.G., Saucedo, J., and Pridmore, C.L., 2002, Geologic map of the Monterey 30' × 60' Quadrangle and adjacent AREAS, California: California Division of Mines and Geology, scale 1:100,000.
- Watson, F., Anderson, T., Casagrande, J., Kozlowski, D., Newman, W., Hager, J., Smith, D.P., and Curry, R., 2003, Salinas Valley Sediment Sources: Seaside, California, Central Coast Watershed Studies Report No. WI-2002-10 to the California Central Coast Water Quality Control Board, 193 p.
- Xu, J.P., Noble, M.A., and Rosenfeld, L.K., 2004, In-situ measurements of velocity structure within turbidity currents: *Geophysical Research Letters*, v. 31, p. L09311.

MANUSCRIPT RECEIVED BY THE SOCIETY 20 OCTOBER 2003

REVISED MANUSCRIPT RECEIVED 2 DECEMBER 2004

MANUSCRIPT ACCEPTED 4 JANUARY 2005

Printed in the USA